Defence Science Journal, Vol. 71, No. 4, July 2021, pp. 524-534, DOI : 10.14429/dsj.71.15947

Designing a Cavity Backed Microstrip Antenna with Enhanced Isolation for the Development of a Continuous Wave Ground Penetrating Radar

Krishnendu Raha* and K.P. Ray

DRDO-Defence Institute Of Advanced Technology, Pune - 411 025, India
**E-mail: krishraha@gmail.com*

ABSTRACT

This paper presents an improved design of a rectangular microstrip antenna at 920 MHz by backing it with an appropriate cavity wall to enhance the isolation between the transmitter and receiver antenna for use in applications, where the weak received power gets masked by the direct coupled power between two antennas. Antennas having 0.12 λ cavity wall with separation gap of 0.36 λ resulted in an isolation of 52.6 dB at a resonance frequency of 920 MHz with maximum and minimum isolation of 71.4 dB and 49.1 dB, respectively for 5% BW of the antenna designed. These antennas were fabricated and tested, which are used in the development of Continuous Wave Ground Penetrating Radar with an online graphical user interface; leading to the validation of the usefulness of proposed antennas. The isolation achieved at an optimised separation of the antennas enabled detection of metal targets as small as a bunch of wire buried 20 cm in the soil and non-metal, like wood and plastic buried in soil. It enabled the detection of a circular steel target of radius 12.5 cm buried at a depth of 65 cm in loose semi-dry pebbled soil.

Keywords: Rectangular microstrip antenna; Cavity backed antenna; Enhanced isolation; Continuous wave ground penetrating radar; Through the wall radar

1. INTRODUCTION

The prime characteristics of antenna design for applications, where the continuous wave is used and the received power is very low are; high gain, high bandwidth, high efficiency and mainly high isolation between the transmitting and receiving antennas. For example, in bi-static continuous wave ground penetrating radar (CW GPR) and through the wall radar (TWR), isolation between the antennas must be high so that coupled power between antennas is smaller than the reflected power received from the buried/hidden target[1]. Isolation between the transmitter (Tx) and receiver (Rx) antennas determines the cleanliness of raw data obtained from the reflected power received from the hidden target. The cleanliness of raw data determines the usefulness/accuracy of signal processing applied on the same for obtaining accurate information/pseudo image.

The receiver sensitivity of GPR/TWR is in the order of -90 to -110 dBm[2] and thus in absence of mutual coupling, antennas are capable of detecting very low power reflected from the target hidden at a depth determined by the frequency of operation and the soil/wall parameters. However, if the isolation between the transmitting and receiving antennas is not high, comparably higher mutual coupling power may mask the low power reflected by the target well before the sensitivity of the system is reached. Thus, the depth to which a particular target can be detected is determined by the isolation between the antennas until the isolation makes the mutual coupling between the antennas comparable to the sensitivity of the receiver system. Changing the transmitted power does not alleviate this issue, because on increasing the transmitted power the corresponding mutual coupling also increases and on decreasing the transmitted power, the power reflected from the target decreases proportionately. Thus, better the isolation, more is the depth of detection for a particular target.

To achieve high isolation between the co-located antennas, generally, they are separated by λ/2 distance and space in-between is filled by radiation absorbing material[3]. The RF radiation absorbing material gives isolation of about 40 dB, but is rather expensive. Alternative ways to increase isolation by creating a spatial notch at the position of the receiving antenna by adding an additional antenna, has been explored in[4]. Maximum isolation of 50 dB has been achieved using this method. However, this design is complex and the level of isolation depends on how accurately the phase and amplitude in the setup can be matched to the designed values. For Patch antennas, in[5-7] electromagnetic band-gap structures; i.e., the printing of various patterns on or within the substrate, have been used to enhance isolation.[8-10] proposes etching of structures on ground plane known as defected ground structure (DGS) to increase isolation. In[11], a ladder shaped conducting wall structure has been used between two closely placed microstrip antennas (MSAs) to enhance isolation up-to 50 dB at 4.45 GHz. But these methods can only be used when transmitting and receiving antennas are printed on the same substrate. When the MSAs are printed on a different substrate, various structures have been placed in between them to enhance isolations, such as in[12], rectangular loop resonators, in[13], a microstrip patch element and in[14], inverted U-shaped resonators. These techniques provide isolation of maximum 44

Received : 09 June 2020, Revised : 12 November 2020
Accepted : 18 February 2021, Online published : 01 July 2021

dB[14] for a compact structure. In line with the above-mentioned generalised methods, for the specific application of TWR/GPR, various methods to enhance isolation between antennas have been explored in the literature. In[15], an optimised rectangular patch antenna operating in the frequency range from 0.5 – 2 GHz with a metal patch placed in-between to improve the performance has been presented. These antennas reported coupling of -15 dB for the antenna separation of 0.83 λ_0. In[16], UWB directional Vivaldi antenna operating at the frequency range of 1.17 - 4.75 GHz is discussed, wherein the mutual coupling between Tx and Rx antennas of - 42 dB has been achieved by either adding metallic plate in-between them or by placing the antennas perpendicular to each other. Presents[17] a metamaterial cavity backed antenna and achieves 50 dB isolation. However, due to the use of metamaterial, this has an inherent narrowband operation. To achieve isolation up to 60 dB at 3.4 GHz, Quadrifilar Helical antennas with Tx having left hand circular polarisation and Rx having an opposite sense of right-hand circular polarisation have been presented in[18]. Though very high isolation has been achieved, the drawback of this design is reduced gain due to the use of circular polarised antenna and the relatively bulky structure due to the use of a helical antenna, which limits its usefulness. In[19], a planar circular symmetric structure in a circularly polarised cross dipole antenna is proposed to reduce mutual coupling by reducing surface waves. At 1.8-7.1 GHz, maximum isolation of 48 dB and gain of 9 dB has been achieved by this method. This literature review brings out a gap in antenna design of not having high mutual isolation (> 50 dB) in non-cross polarised scenarios, particularly for WTR/GPR applications.

This paper presents an innovative way of enhancing isolation (>50 dB) between antennas by putting an appropriately sized cavity wall surrounding the Rectangular Microstrip Antenna (RMSA) and keeping them separated at an optimum distance. The noble concept utilised is that by placing an appropriately sized structure between two identical transmitter and receiver antennas, two coupling paths get created between them. With an optimised height of the cavity rim at a given separation between antennas, comparable electric fields from two paths are made out of phase (180^0), cancelling each other which leads to maximum isolation between them. This concept of the appropriate structure has been explained in[11,20], however, stress is on presenting the structure and not optimising the separation between antennas to obtain maximum isolation and thus only 20 dB isolation was reported[20]. The concept of the rectangular cavity to suppress back radiation is presented in[21-23]. In[21,22], a rectangular cavity surrounds a magneto electric dipole to improve front to back ratio (FTBR) while in[23], a mix of RF absorber and cavity wall suppresses back radiation up to 30 dB in the designed 900 MHz GPR. These papers focus on improving FTBR and suppressing back radiation but are silent on the isolation issue. In the proposed novel design, these two methods, as utilised in[11,20] and[21-23] are combined to obtain very high isolation. Proposed RMSAs are fabricated and tested. Utilising the proposed antennas, a compact portable CW GPR with an online graphical user interface has been designed. The developed system has been tested extensively to demonstrate the capability of the antennas proposed.

The paper is organised into six sections. Following this introduction section, section 2 covers the simulation and fabrication of a simple rectangular Microstrip antenna (RMSA) and RMSA with acavity wall, illustrating the improvement achieved by placing the cavity wall. Section 3 is devoted to the validation/use of the fabricated RMSA with cavity wall in the CW GPR system designed for this purpose. Section 4 gives the results of various experiments conducted using the GPR system with the designed antennas. Section 5 analyses and discusses the results obtained. Finally, conclusions are drawn in section 6.

2 DESIGN OF A RECTANGULAR MICROSTRIP ANTENNA (RMSA)

In order to validate the concept of enhancing isolation of Microstrip antenna by cavity wall of appropriate height with appropriate ground plane and separation between the antennas, the simple configuration of a Rectangular Microstrip antenna has been chosen. IE3D software has been used for simulations. The starting dimensions for antenna resonant at 920 MHz were obtained from formulations given in [24]. Simulated structure of the antenna is at Fig 1. Dimensions of design parameters are at Table 1.

Table 1. Dimension of Design Parameters

Parameters	Dimension (mm)	Remarks
a	195	Square Ground Plane
b	135	Square Radiating Patch
h	14	Gap
x	41	Feed Point (from centre)

The simulated return loss, total efficiency, VSWR, gain versus frequency plots and far field radiation patterns of the antenna are depicted in Fig. 2. The simulated efficiency of 96% with S_{11} of -21.17 dB and gain of 8.57 dB is obtained at resonance frequency of 920 MHz. The bandwidth (BW) corresponding to VSWR<2 is 46 MHz (900 to 946MHz) i.e. 5%. The narrow band design is chosen for effective concept validation of enhancement of isolation by the cavity wall. BW and gain may be increased by using multilayer configuration as in Electromagnetically Coupled Microstrip Antenna (EMCA)[25].

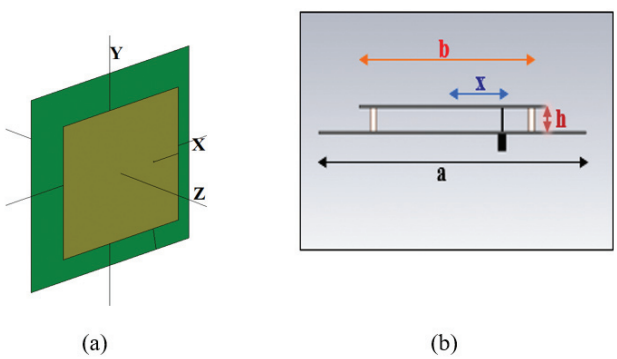

Figure 1. Simulated Structure of RMSA (a) Perspective view and (b) Side view Geometry.

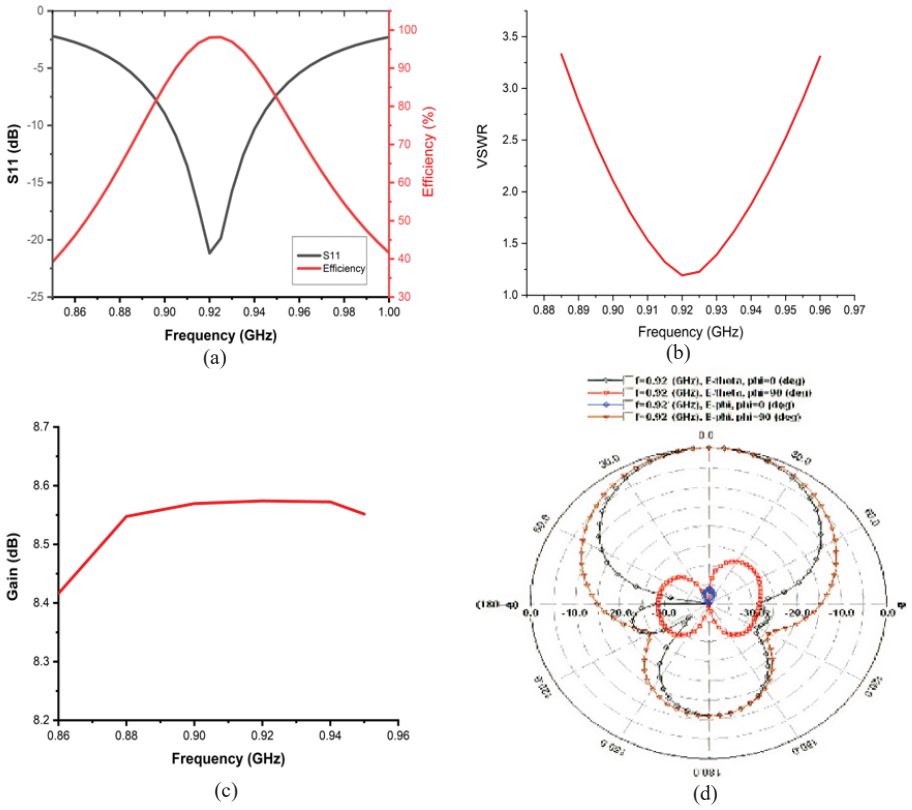

Figure 2. Simulated Plots for RMSA (a) Return loss and Efficiency and (b) VSWR (c) Gain V/s Frequency (d) Far field radiation patterns.

Isolation, i.e., S_{21} between these transmitting and receiving antennas at various separation between them are depicted in Fig. 3. Figure 3(a) depicts the simulated structure of the antenna. Isolation of 40 dB was obtained, when the separation is increased to 300 mm ($0.92\lambda_0$) as evident from Fig 3(b). This value of isolation is not enough and also large separation between the antennas is not acceptable because it will increase the size of the system and more importantly it will not be able to detect small targets.

2.1 RMSA with Cavity Wall

Simple design of RMSA did not yield improved isolation between two antennas. It is envisaged that by developing a cavity of appropriate height on the ground plane around the patch and keeping the antennas separated at optimum gap, high isolation due to destructive interference as discussed earlier, is achieved. Thus, a square cavity is formed by building the square rim centring patch keeping the parameters of the antenna same as given in Table 1. The simulated structure of RMSA with cavity wall is presented in Fig. 4. Comparison of return loss, total efficiency, VSWR and the gain of RMSA with and without cavity wall is presented in Fig. 5(a) to 5(c). Far field radiation patterns of the RMSA with cavity wall is given in Fig. 5 (d). Effects of cavity wall on these parameters are discussed in section 2.2.1.

Exhaustive simulations have been carried out to determine isolation between two antennas by varying separation (x) and the cavity height (h). Schematic diagram of two cavity backed

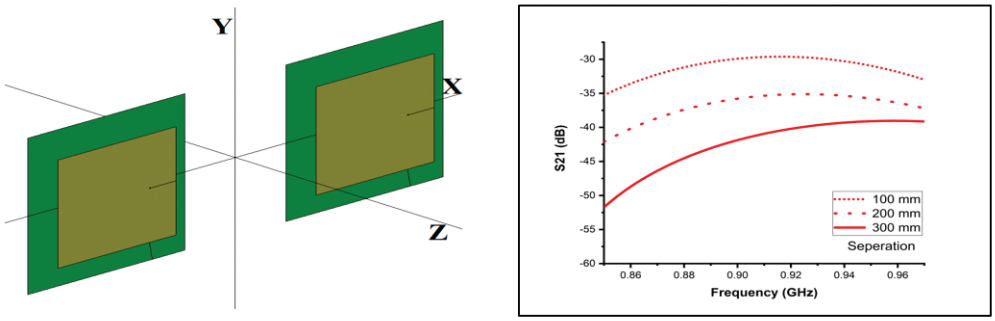

Figure 3. Isolation (S_{21}) for different Separating Gaps of RMSAs (a) Simulated structure of two RMSAs with separation of x for isolation measurement (b) Isolation (S_{21}) at various separating gap of RMSAs.

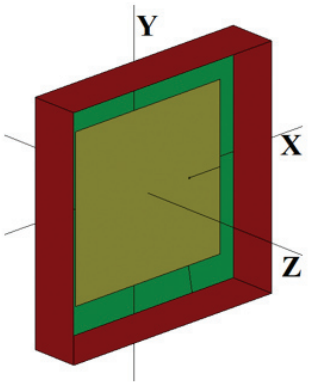

Figure 4. Simulated Structure of RMSA with Cavity wall.

RMSA with separating distance for simulation of isolation is shown in Fig.6. Results of the simulation study are given in Table 2 and Table 3, respectively.

From the tables, it is noted that maximum isolation is obtained only at a particular height of the cavity wall and for a particular separation. For the separation of x=120 mm and with the cavity height of h=40 mm the isolation obtained is 54.6 dB. It is stressed that, the isolation is not enhanced either by increasing or decreasing the separation (of 120 mm) nor by changing the optimum cavity height (40 mm) for 120 mm gap. It is, therefore, inferred that destructive interference between direct and scattered radiation from the cavity rim yields maximum isolation for this combination of cavity height and separation between two antennas at the operating wavelength.

Table 2. Isolation between Transmitting and Receiving Antennas with varying Separation (x) between them with a fixed Cavity Height (h) of 40 mm at 920 MHz.

x (mm)	S_{21} (dB)
30	-35
60	-41.1
90	**-52**
110	-52.5
116	-52.5
120 (0.36 λ)	**-54.6**
130	-51.26
150	-50
210	-47.3
240	-46.8
270	-46.5

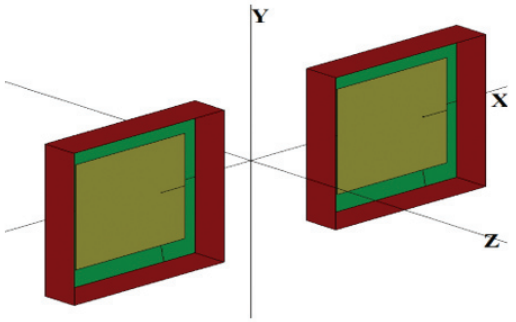

Figure 6. Simulated Structure of two Cavity Backed RMSAs with Separation of x for Isolation Measurement.

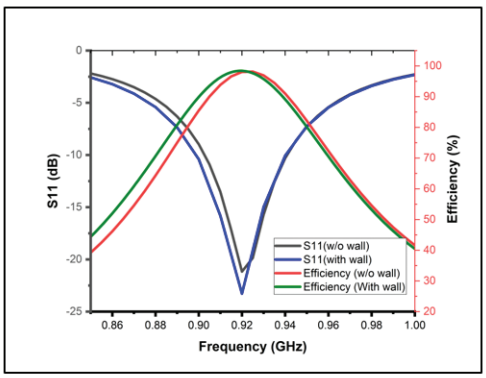

(a)

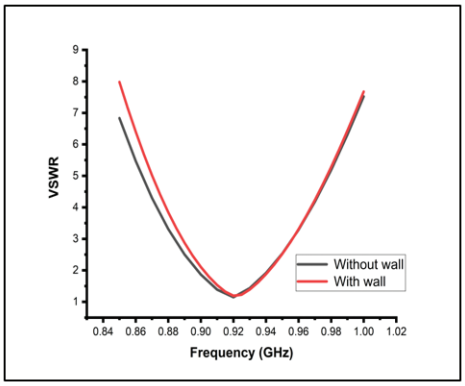

(b)

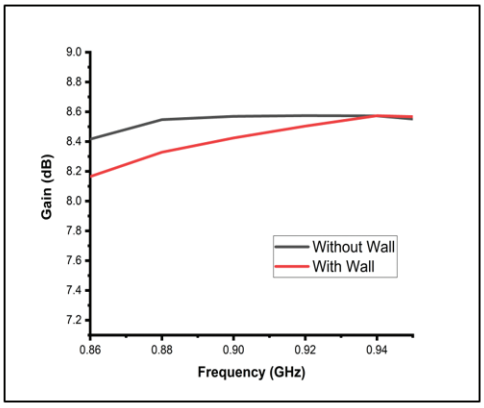

(c)

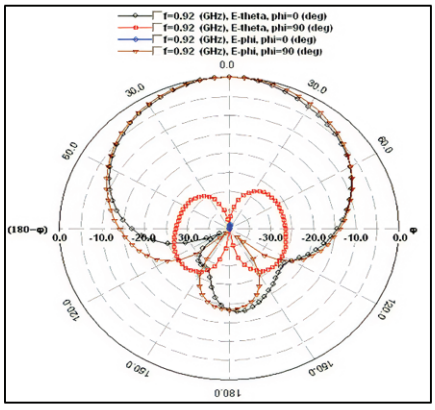

(d)

Figure 5. Simulated Plots (a) to (c) Comparing with Cavity and without Cavity RMSA (a) Return loss and Total Efficiency (b)VSWR (c) Gain V/s Frequency (d) Far field radiation patterns of Cavity wall RMSA

Table 3. Isolation between Transmitting and Receiving Antennas with fixed separation (120 mm) between them with a varying Cavity height (h) at 920 MHz.

h (mm)	S_{21} (dB)
20	-33.7
26	-36.5
30	-39.9
40 (0.12 λ)	**-54.6**
41	-50
42	-47.4
43	-45.3
50	-37
60	-32.2
80	-28.04
100	-27.4

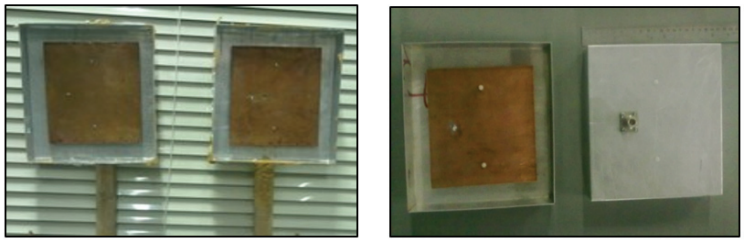

Figure 7. Photographs of Prototype Cavity backed RMSAs.

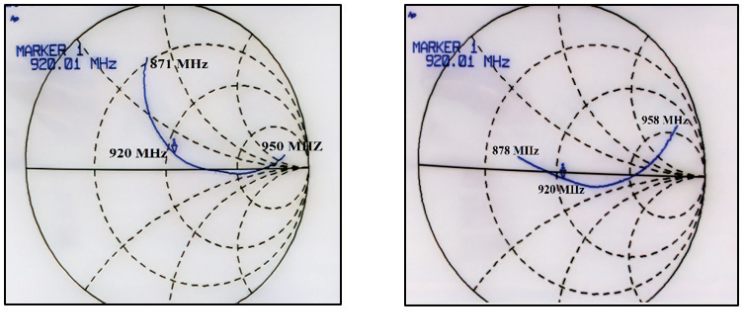

(a) (b)

Figure 8. Screen Captured plots from Network Analyzer of Impedance loci in Smith Chart (a) Transmitting Antenna and (b) Receiving Antenna.

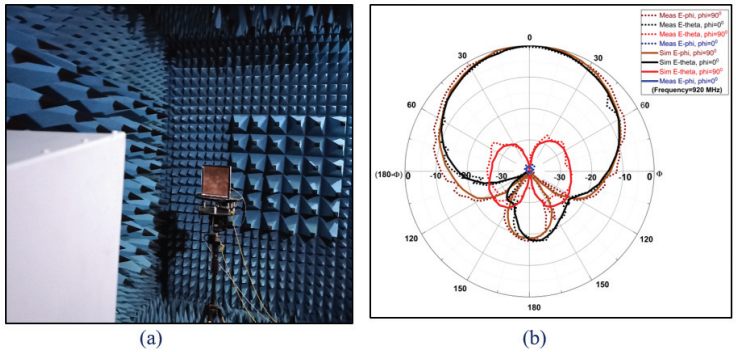

(a) (b)

Figure 9. Radiation Patterns for Cavity Backed RMSA (a) Anechoic Chamber Setup (b) Comparison of Measured and Simulated Result.

2.2 Fabrication and Measurement of RMSAs with Cavity Wall

Prototype transmitter and receiver cavity backed RMSAs, as shown in Fig. 7, were fabricated using a copper plate suspended in the air with two Teflon supports at the centre line and an aluminium plate as the ground plane. Both these antennas have been tested for the input matching. Both these antennas yielded similar results. While carrying out measurements using Network Analyzer, the screen captured plots of impedance loci in Smith Chart of both the transmitting and receiving antennas are depicted in Fig. 8. Comparison of measured and simulated radiation patterns is shown in Fig. 9(b) and Anechoic Chamber setup for this measurement is given in Fig. 9 (a). Comparison of measured and simulated VSWR is presented in Fig 10. Comparison of measured and simulated isolation at 120 mm separation covering the BW of the antenna is depicted in Fig. 11. The line-of-sight S_{21} measurements have been carried out indoor using a two-port network analyser with one port of the network analyser connected to the transmitting antenna while the other to the receiving antenna. Measured results are in good agreement with simulations.

2.2.1 Effects of Cavity Wall

Placing cavity wall has a negligible effect on total efficiency, return loss, BW & gain of the RMSA as evident from comparison graphs in Fig. 5.

Simulated radiation patterns of RMSA without and with cavity wall have been presented in Fig. 2 (d) and 5 (d) respectively and the measured radiation patterns of RMSA with cavity wall have been compared with simulated ones in Fig. 9 (b), which are in good agreement. For both with and without cavity wall cases, it is noted that HPBW in both E and H planes are approximately 50^0, indicating that gain of both the antennas is comparable. Notably, placing the cavity makes the radiation patterns of the antenna in E-plane and H-plane more symmetrical as depicted in Fig. 5 (d) & 9. Additionally, the front to back ration (FTBR) of 20 dB is obtained for the cavity backed antenna, which is an improvement of around 10 dB over the antenna without a cavity.

It is depicted in Fig.11 that there is an improvement of 25 dB in the value of isolation at 920 MHz, when a cavity is put around RMSA. For RMSA without cavity wall, isolation of 40 dB was obtained for simulated separation of 300 mm **(0.83** λ) between the antennas and RMSA with cavity wall isolation of 54.6 dB was obtained for a simulated separation of 120 mm **(0.36**λ). Measured isolation with and without cavity wall for 120 mm separation is 52.6 dB and 27.5 dB, respectively. Within 5% designed BW, cavity backed RMSA provided maximum isolation of 71.4 dB and minimum of 49.1 dB whereas without cavity wall RMSA provided a maximum isolation of 29.5 dB and minimum of 27.5 dB.

These comparisons establish the benefits of putting cavity wall in RMSA which are desirable for TWR/GPR applications.

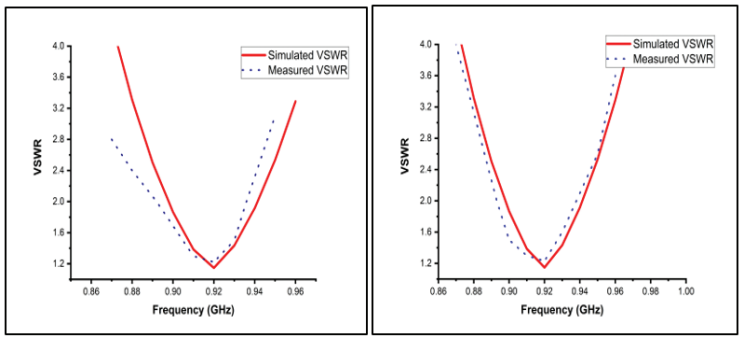

Figure 10. Comparison of Measured and Simulated Results of VSWR for Cavity Backed RMSA (a) Transmitting Antenna and (b) Receiving Antenna.

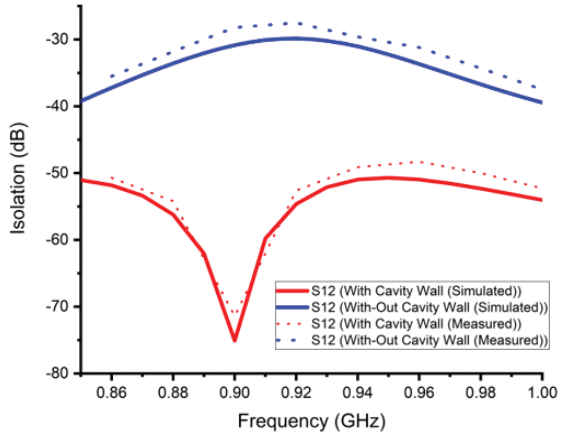

Figure 11. Comparison of Measured and Simulated Isolation at 120 mm Separation of Cavity Backed RMSA for a Cavity Wall Height of 40 mm.

3. VALIDATION/USE OF CAVITY BACKED RMSA IN GPR SYSTEM

A compact portable laboratory model of CW-GPR [26] has been made by using proposed antennas with enhanced isolation. Extensive experimental trials have been conducted using the CW-GPR system which in turn validates and demonstrates the usefulness of the antenna designed. The CW-GPR module extracts the amplitude and phase information from the signal reflected from the target using AD 8347 I/Q demodulator[27], which is the main part of the module. The I and Q data of the reflected signal are passed through a low pass filter designed with a cut off frequency at 20 Hz and then fed to the A/D converter. Open-source Arduino Uno module has been used as A/D converter. Code has been written to extract analogue I and Q data and display the converted digital data. GUI interface of open-source Arduino has been used to write these codes.

3.1 Designing a Compact Portable CW GPR System

A single PCB has been designed for the transmitter, receiver and microcontroller so as to make the system compact. The PCB is fabricated on a 1.6 mm FR-4 substrate with ε_r= 4.4 and tanδ = 0.02. The PCB designed along with all the components soldered is depicted in Fig.12 (a). Fig.12 (b) depicts Ardiono Uno (micro controller) and the 6 V DC, 48 AH battery connected to the PCB.

Antennas are placed close to the ground at the base of the product as shown in Fig. 13 (a). The final product designed is shown in Fig. 13 (b).

3.2 Online Graphical User Interface (GUI) Design

For displaying amplitude and phase information of the target detected in real time a graphical programming environment (LabVIEW) has been used. LabVIEW design software has been integrated with Arduino[28] and a user-friendly GUI has been designed as depicted in the result section, to demonstrate the results. GUI designed has the capability to calibrate the system according to soil condition, fine tune the frequency, and control the overall gain of the receiver.

3.3 Experimental Setup

Extensive experiments have been carried out with the final GPR system. Experimental setup with air as host medium is given in Fig. 14 (a). Experimental setup, where various targets buried in soil and the product has been moved over the soil is depicted in Fig.14 (b). Transmitted power used is -10 dBm for all the experiments. Selective experiments and result obtained are illustrated in the subsequent section.

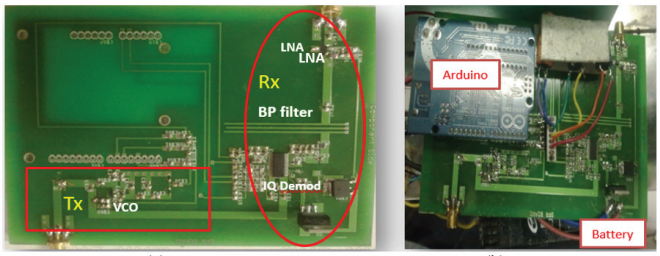

Figure 12. PCB design (a) Components soldered and (b) Ardiono and Battery connected.

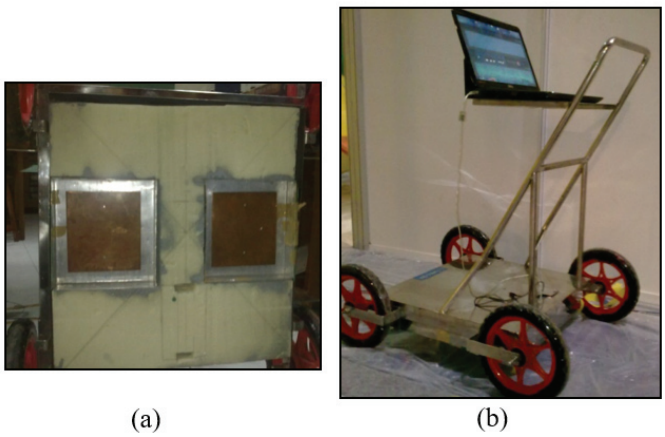

Figure 13. CW GPR Prototype (a) Front face of the base consisting of antennas designed (b) Prototype with antennas, PCB and power module at the base close to the ground and the display unit close to the user.

(a) (b)

Figure 14. Experiment Setup (a) With air as host medium (b) Targets buried in soil.

4. EXPERIMENTAL RESULTS

4.1 Results of Experiments with air as Host Medium

First set of experiments were performed with various objects in air, which are discussed in following section.

4.1.1 Metallic Targets of Different Size and a Wooden Slab at same Depth

Different size metal plates including a circular steel plate of diameter 25 cm, a circular aluminium plate of diameter 20 cm, a rectangular aluminium plate of side 10 cm and a square wooden slab of side 25 cm have been moved below the product one after the other (in the order as specified here). All these objects were kept at same depth of 50 cm below antennas with air as host medium. Results obtained are depicted in Fig. 15. It is seen that as the metal plate size decreases the corresponding received amplitude peak decreased (as the power reflected from it decreases). It is to be noted that because all the three metallic targets are in same depth, the phase pattern obtained is same for all of them. However, there is a difference in width of the pattern in both in amplitude and phase because the targets have been moved at different speed. For the same depth, using the moist wooden target, the amplitude valleys and a dip is obtained. This is because of absorption of EM radiation by moist wood. It is noted that even a very weak reflected signal is detected because of high isolation between transmitting and receiving antennas.

4.2 Experiment with Targets Buried in Soil

For the actual functioning of GPR, various targets were buried in the ground. First experiment was carried out to establish the maximum depth of detection of the GPR outside laboratory in semi dry soil followed by detection of a plastic box and detection of a small bunch of wire buried in soil.

4.2.1 Experiment to Determine Maximum Depth of Detection of the GPR

To get a rough idea about maximum depth of detection of the product, experiment as depicted in Fig.16 (a), has been carried out. A circular steel target of diameter 25 cm was buried in loose semi-dry soil with lots of small pebbles in it. The figure shows the target exposed but it has been buried in soil during experiment such that depth of soil over the target is about 65 cm. Next, the product has been moved over the soil heap. Fig. 16 (b) depicts the detected signal. With no target present, the detected amplitude level varies from 0.3V to 0.8V. This variation is because of the presence of many small pebbles in the soil. When the product moves and reaches the location below which the target is buried, the received amplitude become stable at the level of 1V. After this as the product is moved away from the target the amplitude level again starts varying. Also, it is noted that because the target is

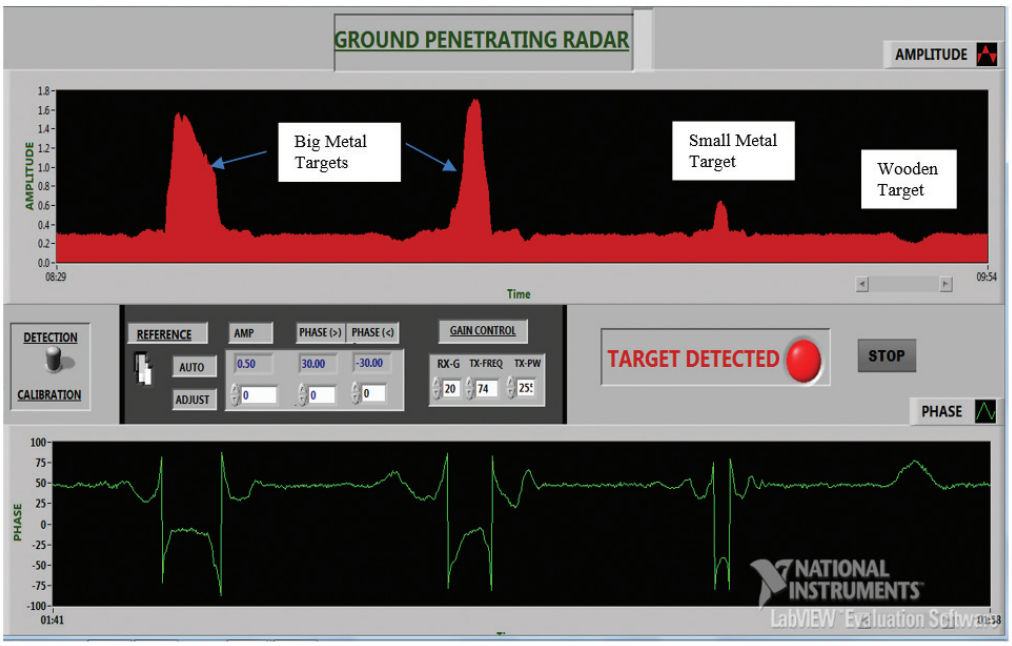

Figure 15. Received Signal from Metallic Targets of different size and a Wooden slab at same Depth in air medium.

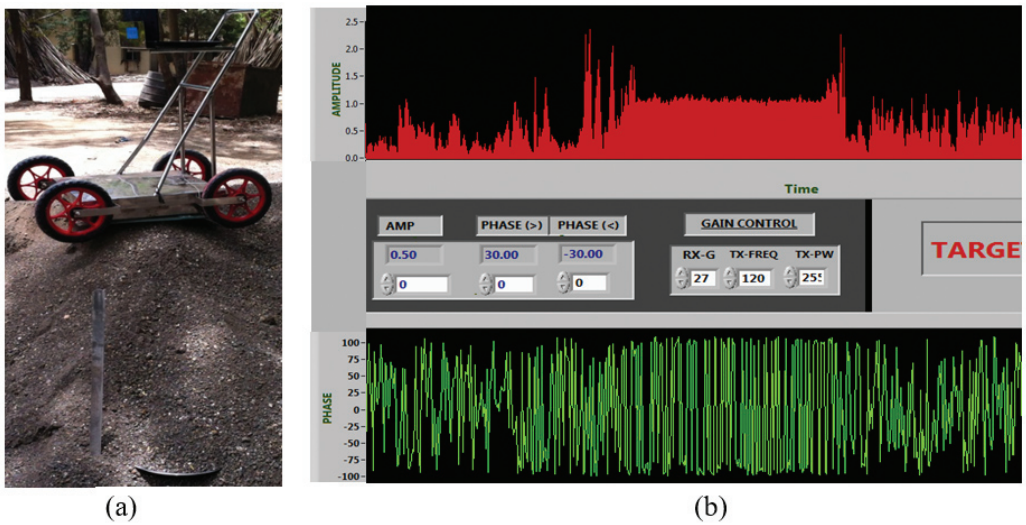

Figure 16. Determining the Maximum Depth of Detection of the GPR (a) Experiment setup (b) Detection of target at depth of 65 cm in soil.

buried so deep and the target size is not so big, amplitude level detected as compared to the reference level (ie. when no target is present) is not much different (only it is more stable) and no phase information about the target is obtained. It is inferred that the GPR cannot detect target smaller than the present one beyond the depth of 65 cm in this type of soil.

4.2.2 Detecting a Plastic Box and a Bunch of Wire Buried in Soil

A small plastic box of size 15 x 10 x 3 cm^3 and a bunch of wire have been used as targets and placed at a depth of 20 cm inside the soil. Fig.17 (a) depicts the result obtained using GPR for plastic box target. The high reflected power obtained here is on account of difference of dielectric constant of air (trapped in the plastic box) and dielectric constant of the soil. Fig. 17 (b) depicts the result for detecting bunch of wire. In this case the reflected power is not stable because it's a bunch of wire i.e. it consists of many small plastic-coated copper wires with soil in between and is not a monolithic big target.

5. ANALYSIS OF THE RESULTS AND DISCUSSIONS

The prototype of CW GPR, which has been designed incorporating the proposed antenna with enhanced isolation, successfully detected metal targets as small as a bunch of wire buried 20 cm in the soil and non-metal like wood and plastic buried in soil. For a metallic circular plate of diameter 25 cm buried in semi dry pebbled soil, experiments have been carried out for successful detection up to the depth of 65 cm for low transmitted power (-10 dBm). It is imperative that, from the measured phase and amplitude information, the depth of the target can be ascertained[23].

This paper highlights the novel method of enhancing the isolation of an RMSA for a sensitive GPR system. Table 4 compares related work with the proposed work.

In Table 4, reference[3,14] separating gap between the antennas is 0.5 λ while this work achieves the claimed isolation at 0.36 λ separation[4,14] is complex in design while the proposed work is based on simple cavity backing of RMSA[14,17]

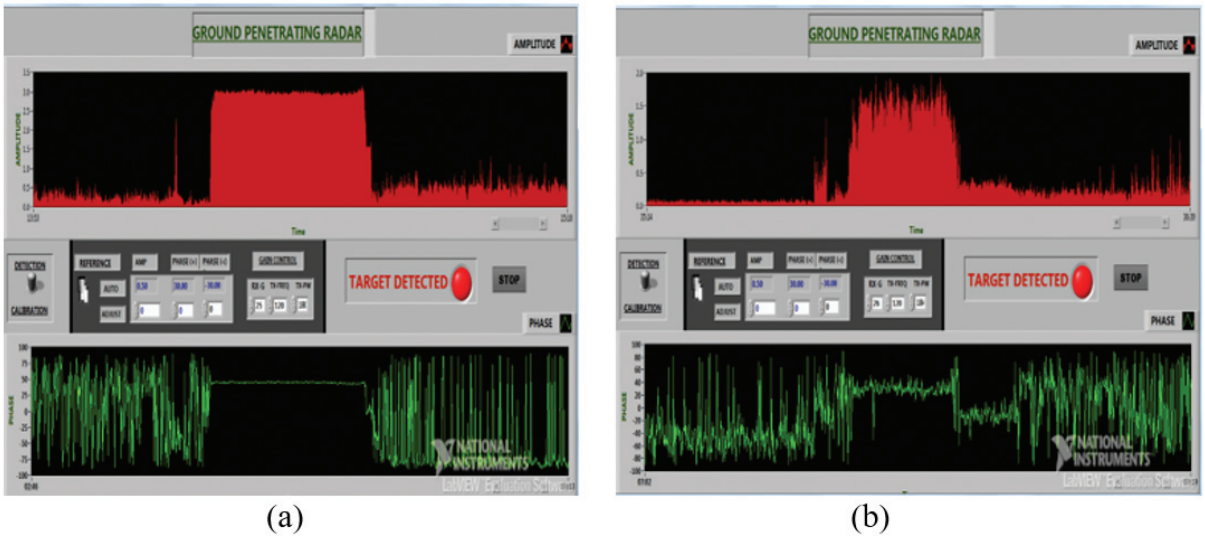

Figure 17. Received Amplitude and Phase Response of Target buried 20 cm in Soil (a) Plastic Box (b) Bunch of Wire.

Table 4. Comparison with Related Works

Ref	Freq. Range (GHz)	Isolation Method	Max Isolation (dB)	Comments
[03]	9-11	RF absorber	40	Cost prohibitive
[04]	2.5	Spatial notch	50	Complex Design
[14]	5.125-5.375	Resonator between antennas	44	Narrowband & complex
[16]	17-4.75	Metallic plates between antennas	42	Isolation less than 50 dB
[17]	2.5–2.7	Metamaterial cavity	50	Inherent Narrow band
[18]	3.4	Circular polarised helical antenna	60	Low gain
[19]	1.8-7.1	Circular polarised cross dipole	48	Isolation less than 50 dB
Prop.	**0.90 - 0.946**	**Cavity backed RMSA at optimised separation**	**71**	**High Isolation & Simple Design**

are inherently narrowband because of the use of U-shaped resonator and metamaterial cavity respectively, while the work proposed can be extended to wide band ECMA[25], obtains[18] 60 dB isolation at relatively higher resonance frequency and using cross polarisation which makes it low gain. In comparison, the proposed antenna has 8.5 dB gain with isolation of 52.6 dB at resonance frequency of 920 MHz. In[19], maximum isolation of 48 dB is obtained in the wide BW of 5.3 GHz, while the present work gives maximum isolation of 71 dB in narrow BW of 45 MHz. The isolation obtained may be further increased by adding RF absorbent between the antenna.

In this work, a single frequency CW GPR concept has been used to demonstrate the capability. However, to find out the exact depth and pseudo image of the buried target a band of frequencies would be required[29,30] so that more information about the target is available and accordingly antenna may be re-designed to cater for the broad BW requirement, which could be realised using EMCA[25]. The broad BW will also enable required resolution in detecting targets. To obtain required isolation for broad BW, a double wall cavity structure, each targeting a particular BW span and a mix of RF absorbent material[23] may be utilised. The isolation achieved will enable detection of target at a greater depth using the same frequency and provide cleaner raw data for applications like GPR/TWR which will be instrumental in better signal processing. For example, in GPR the cleaner raw data will enable finding out better information about the target like detecting exact depth/ forming pseudo image[30,31]. While in TWR the cleaner raw data will assist in extracting cleaner heart beat signature, which when categorised by Support Vector Machines or Convolution Neural Network will be able to provide intent of the target hiding behind the wall [32, 33].

6. CONCLUSION

An innovative technique of surrounding the RMSAs with 0.12 λ cavity wall and placing them at 0.36 λ separation resulted in maximum isolation of 71.4 dB and minimum of 49.1 dB for 5% BW at the resonance frequency of 920 MHz. A portable compact low-cost CW GPR system has been fabricated using the proposed antennas with an online GUI. The same has been used to demonstrate the capability of the proposed antennas by detecting weak signal from less reflecting buried objects. The designed antenna caters to a single frequency of operation, however for multi frequency operations used in practical cases, antennas may be appropriately modified to cater for the bandwidth requirement and a judicious use of absorber and cavity wall technique may be applied to obtain better isolation for wide bandwidth.

REFERENCES

1. Ida, N. & Meyendorf, N. Handbook of advanced non-destructive evaluation. Springer International Publishing, USA, 2019. pp. 1-38. doi: 10.1007/978-3-319-30050-4_9-1
2. Seyfried, D.; Schubert, K. & Schoebel, J. Investigations on the sensitivity of a stepped-frequency radar utilizing a vector network analyzer for Ground Penetrating Radar. *J. Appl. Geophy.,* 2014, **111**, 234-241. doi: 10.1016/ j. jappgeo.2014.10.01
3. Channabasappa, E. & Egri, R. System and method of using absorber-walls for mutual coupling reduction between microstrip antennas or brick. US patent 7427949B2, 23 September 2008.
4. Janssen, E.; Milosevic, D.; Herben, M. & Baltus, P. Increasing Isolation bet-ween Co-located Antennas using a Spatial Notch. *IEEE Antennas Wirel. Propag. Lett.,* 2011, **10**, 552-555. doi: 10.1109/LAWP.2011.2158510
5. Li, L.; Yu, Y. & Yi, L. Mutual coupling reduction between printed dual-frequency antenna Arrays. *Pro. Electromag. Res. Lett.*, 2016, **59,** 63–69. doi: 10.2528/PIERL16020601
6. Zhai, G.; Chen, ZN. & Qing, X. Mutual coupling reduction of a closely spaced four element MIMO antenna system using discrete mushrooms. *IEEE Trans. Microw. Theor. Techniq.*, 2016, **64**(10), 3060-3067. doi: 10.1109/ TM- TT. 2016. 2604314
7. Najam, A.I.; Duroc, Y.; Leao, J.F. & Tedjin, S. A novel co-located antennas system for UWB-MIMO applications. *In* IEEE Radio and Wireless Symposium, 2009. doi: 10.1109/RWS.2009.4957357
8. Toolabi, M.; Sadeghzadeh, R.A. & Nasser-Moghadasi, M. Compact meandered-shape electromagnetic bandgap structure using in a microstrip array antenna application. *Microw. Optical Technolo. Lett.,* 2016, **58**(9), 2084-2088. doi: 10.1002/mop.29982
9. Prahlada Rao, K.; Vani, R.M. & Hunagund, P.V. Two element microstrip antenna array using star slot

electromagnetic band gap structure. *Int. J. Eng. Sci.*, 2019, **26**(4), 78 – 87.
doi: 10.5281/zenodo.3591584.

10. Park, C.H. & Son, H.W. Mutual coupling reduction between closely spaced microstrip antennas by means of H-shaped conducting wall. *Electron. Lett.,* 2016, **52**(13), 1093-1094.
doi: 10.1049/el.2016.1339.
11. Alsultan, R.G. & Yetkin, G.Ö. Mutual coupling suppression of closely spaced microstrip antennas by ladder-shaped conducting wall. *Int. J. Commun. Syst.*, 2018.
doi: 10.1002/dac.3798
12. Ketzaki, D.A. & Yioultsis, T.V. Metamaterial-based design of planar compact MIMO monopoles. *IEEE Trans. Anten. Propaga.*, 2013, **61**(5), 2758-2766.
doi: 10.1109/TAP.2013.2243813
13. Babu, K.J.; Aldhaheri, R.W.; Younus, T.M. & Alruhaili, I.S. Design of a compact two element MIMO antenna system with improved isolation. *Pro. Electromag. Res. Lett.,* 2014, 48, 27-32.
doi: 10.1023/A:1008889222784
14. Ghosh, C.K. A compact 4-channel microstrip MIMO antenna with reduced mutual coupling. *Int. J. Electron. Commun (AEÜ).*, 2016, **70**(7), 873-879.
doi: 10.1016/j.aeue.2016.03.018
15. Fioranelli, F.; Salous, S.; Ndip, I. & Raimundo, X. Through-the-wall detection with gated FMCW signals using optimized patch-like and Vivaldi antennas. IEEE Trans. Anten. Propaga., 2015, **63** (3), 1106-1117.
doi: 10.1109/TAP .2015. 2389793
16. Tahar, Z.; Derobert, X. & Benslama, M. An Ultra-Wideband Modified Vivaldi Antenna Applied to Through the Ground and Wall Imaging. Progress in Electromagnetics Research C., 2018, 86, 111-122.
doi: 10.2528/pierc18051502
17. Li, J.; Yang, S.; Wang, C.; Joines, W.T. & Liu, Q. Metamaterial cavity for the isolation enhancement of closely positioned dual-polarized relay antenna arrays. *Microw. Opt. Technol. Lett.,* 2017, **59**(4), 857-862.
doi: 10.1002/mop.30413.
18. Kaur, G. & Ram, S.S. Reduced Coupling for Through Wall Radars Using Orthogonal Circular Polarized Antennas. In IEEE International Symposium on Antennas and Propagation & USNC/URSI National Radio Science Meeting, 2018.
doi: 10.1109/APUSNCURSINRSM.2018.8608433
19. Akbarpour, A. & Chamaani, S. Ultra-Wideband Circularly Polarized Antenna for Near-Field SAR Imaging Applications. *IEEE Trans. Antennas Propag*., 2020, **68**(6), 4218-4228.
doi: 10.1109/TAP.2020.2975097
20. Luo, C.M.; Hong, J.S. & Amin, M. Mutual coupling reduction for dual-band MIMO antenna with simple structure. *Radioengineering., 2*017, **26**(1), 51-56.
doi: 10.13164/re.2017.0051
21. Li, J.; Zhang, A.; Liu, J. & Liu, Q.H. Cavity-backed wideband magneto-electric antenna for through-the-wall imaging radar applications. *In* IEEE RadarConf, 2016.
doi: 10.1109/RADAR.2016.7485327
22. Malhat, H.A. & Zainud-Deen, S.H. Reconfigurable Plasma Circularly Polarized Magneto-Electric Dipole Antenna. *In* 35th National Radio Science Conference, 2018.
doi: 10.1109/NRSC.2018.8354354
23. Chen, G. & Liu, R.C. A 900MHz shielded bow-tie antenna system for ground penetrating radar. *In* Proceedings of the XIII International Conference on Ground Penetrating Radar, Lecce, 2010.
doi: 10.1109/ICGPR.2010.5550125
24. Kumar, G. & Ray, K.P. Regularly Shaped Broadband MSAs. In Broadband Mircrostrip Antenna. Artech House, USA, 2003. pp.30-52.
25. Kumar, G. & Ray, K.P. Multilayer Broadband MSAs. In Broadband Mircrostrip Antenna. Artech House, USA, 2003. pp.131-144.
26. Travassos, X.L.; Avila, S.L.; Adriano, R.D. & Ida, N. A review of ground penetrating radar antenna design and optimization. *J. Microw. Optoelectron. Electromagn. Appl.,* 2018, **17**(3), 385-402.
doi: 10.1590/2179-10742018v17i31321
27. AD8347Datasheet.www.analog.com/static/importedfiles/datasheets/AD8347 .pdf [Accessed on December20, 2019].
28. Community: LabVIEW Interface for Arduino Setup Procedure. https://decibel.ni.com/content/docs/DOC-15971 [Accessed on December 30, 2019].
29. Stickley, G.F.; Noon, D.A.; Cherniakov, M. & Longstaff, I.D. Gated Stepped Frequency Ground Penetrating Radar. *J. Appl. Geophy.*, 2000, **43**(2-4), 259-269.
doi: 10.1016/S0926-9851(99)00063-4
30. Zyada, Z.; Matsuno, T.; Hasegawa, Y.; Sato, S. & Fukuda, T. Advances in GPR-based landmine automatic detection. J. Franklin Inst., February 2011, **348**(1), 66-78.
doi: 10.1016/j.j franklin.2009.02.014
31. Koppenjan, S.K.; Allen, C.M.; Gardner, D.; Wong, H.R.; Lee, H. & Lockwood, S.J. Multi-Frequency Synthetic-Aperture Imaging with a Lightweight Ground Penetrating Radar System. *J. Appl. Geophy*., 2000, **43**(2-4), 251-258.
doi: 10.1016/S0926-9851(99)00066-X
32. Kim, Y. & Ling, H. Human activity classification based on micro doppler signatures using a support vector machine. *IEEE Trans. Geosci. Remote Sens*., 2009, **47**(5).
doi: 10.1109/TGRS.2009.2012849
33. Kılıç, A.; Babaoğlu, İ.; Babalık, A. & Arslan, A. Through-Wall Radar Classification of Human Posture Using Convolutional Neural Networks. *Int. J. Antennas Propag.*, Mar 2019.
doi: 10.1155/2019/7541814

ACKNOWLEDGMENT

Authors would like to record deep sense of gratitude to Prof Girish Kumar, IIT Bombay for the motivation and guidance. Designed antennas and the CW GPR product were tested in his lab at IIT Bombay. Authors would also like to thank Prof Y.V Rao for assisting in making blue print and mechanical designing of the product.

CONTRIBUTORS

Lt Col Krishnendu Raha has received BTech (Electronics and Telecommunication) from Murshidabad College of Engineering & Technology, Kalyani University, India, and MTech (Communication) from Indian Institute of Technology Mumbai, India. He is a serving Indian army signal corps officer with 17 years of experience in counter insurgency, signal intelligence, tactical and strategic Indian army communication. He was part of the team which has planned and commenced the execution of Pan India Army strategic backbone communication network on IP-MPLS. Currently, he is posted as instructor at Military Institute of Technology and is pursuing his PhD at Defence Institute of Advanced Technology, DRDO, Pune, India. His area of research involves: microwave communication systems and antenna designs.

In the current study, after extensive literature survey, he designed the antennas, optimised their performance using simulations, fabricated the antennas and tested their performance. He also fabricated the CW GPR product and designed the online GUI to demonstrate the capability of the designed antennas.

Dr K.P. Ray is MTech in Microwave Electronics from University of Delhi and PhD from Department of Electrical Engineering IIT, Bombay. Presently he is a Professor, Dean Research and head of the Department of Electronics Engineering, Defence Institute of Advanced Technology (DIAT), Pune. He has successfully executed over 46 projects sponsored by Govt. agencies/industries in the capacity of a designer, a chief investigator and a project manager. Has co-authored a book with Prof G. Kumar for Artech House, USA and published over 400 research papers in international/national journals and conference proceedings. He holds 3 patents and filed three patents. He is an associate editor of many International Journals.

In the current study, he conceived the idea to enhance the isolation of Electromagnetically Coupled Microstrip Antennas, finalised antenna specifications, formulated procedure for optimisation of the design, guided in measurements and approved the final result and manuscript.